Published in final edited form as:
*J Neurosci Res*. 2010 November 15; 88(15): . doi:10.1002/jnr.22496.

# Homozygous inactivation of the *Lgi1* gene results in hypomyelination in the peripheral and central nervous system

**Jeane Silva**[1], **Suash Sharma**[1,2], **Bernard Hughes**[1], **Y. Eugene Yu**[3], and **John K Cowell**[1]

[1]MCG Cancer Center, School of Medicine, Medical College of Georgia, Augusta 30912, USA

[2]Department of Pathology, School of Medicine, Medical College of Georgia, Augusta 30912, USA

[3]Department of Cancer Genetics, Roswell Park Cancer Institute, Buffalo, New York, 14263, USA

## Abstract

Mutations in the *LGI1* gene in humans predispose to the development of Autosomal Dominant Partial Epilepsy with Auditory Features (ADPEAF). Homozygous inactivation of the *Lgi1* gene in mice results in an epilepsy phenotype characterized by clonic seizures within 2–3 weeks after birth. Before onset of seizures the 2–3 week-old null mutant mice show poor locomotor activity and neuromuscular strength. EM analysis of the sciatic nerve demonstrates impaired myelination of axons in the peripheral nervous system. Although heterozygous mutant mice do not show any locomotor phenotypes, they also demonstrate an intermediate level of hypomyelination compared with the wild type mice. Hypomyelination was also observed in the central nervous system which, although relatively mild, was still significantly different to the wild type mice. These data suggest a role for LGI1 in the myelination functions of Schwann cells and oligodendrocytes.

### Keywords

LGI1; hypomyelination; mutant null mouse; CNS; PNS

## Introduction

The process of axonal myelination provides the insulation that axons need to ensure proper propagation of action potentials. The multiple myelin coats on axons are provided by the action of the Schwann cells in the peripheral nervous system (PNS) and the oligodendrocytes in the central nervous system (CNS). These cells wrap layers of myelin around the axons in a process that begins early after birth. Disruption of the myelination process can lead to a number of congenital and acquired diseases that result in a variety of neuropathies (Nelis et al 1999, Scherer and Wrabetz, 2008). The discovery of genes involved in this process provides the opportunity to gain a better understanding of myelination.

The claw-paw phenotype (*clp*) in mice is a recessive condition that results from incomplete myelination in the PNS, causing lethargic movement in *clp/clp* mice as well as the signature deformity involving the hind limbs (Henry et al 1991). Recently, the *Lgi4* gene was shown to be responsible for the *clp* phenotype by compromising the axon-myelinating role of Schwann cells (Bermingham et al 2006). *LGI4* is a member of a highly homologous family of genes that contains a leucine rich repeat (LRR) motif in the N-terminal region of the

Correspondence; John K Cowell, MCG Cancer Center, CN4121, School of Medicine, Medical College of Georgia, 1120 15th Street Augusta 30912, USA.

protein. There are three other members of this family which show different expression patterns in the adult organism (Herranz-Pérez et al, 2010).

In humans, mutations in *LGI1* (Kalachnikov et al 2002) predispose to a rare form of epilepsy known as autosomal dominant partial epilepsy with auditory features (ADPEAF), also referred to as autosomal dominant temporal lobe epilepsy (ADTLE) with onset of seizures occurring as early as 8 years old (Ottman et al 1995). We recently developed a null mutant mouse for the *Lgi1* gene, which also develops early onset seizures (Yu et al 2010). These mice demonstrated increased glutamatergic excitation of presynaptic membranes providing an explanation for the seizure phenotype. The *LGI1* gene encodes a secreted protein (Senechal et al 2005, Sirerol et al 2006, Head et al 2007) that is expressed in a distinct subset of cells in the body (Head et al 2007). The function of LGI1, however, is still poorly understood. Since one member of this gene family has already been shown to be involved in the myelinating role of Schwann cells in the PNS, it is possible that LGI1 may also be involved in this process. During our characterization of the *Lgi1* null mutant mice, which died following seizures at 12–20 days of age (Yu et al 2010), we noted that these mice were also extremely lethargic during the first two weeks of life and showed poor locomotor skills, although they did not show the claw-paw deformity seen in *Lgi4* null mutant mice. To determine whether loss of LGI1 function results in myelination abnormalities, we undertook an extensive analysis of peripheral nerve axon fibers and nerve tracts located in the white matter of the spinal cord. Our analyses demonstrate hypomyelination in the PNS and CNS. In the PNS, hypomyelination is associated with various pathologies suggestive of axonal degeneration.

## MATERIALS AND METHODS

### Electron Microscope analysis

Experimental mice were fixed (4% formaldehyde, 2% glutaraldehyde in 0.1 M sodium cacodylate (NaCac) buffer, pH 7.4) using cardiac perfusion. All surgical procedures were performed under isoflurane inhalation anesthesia according to MCG approved IACUC protocols. To prepare the sciatic nerve, the skin on the right hind-leg of the mouse was removed and the right sciatic nerve was exposed by splitting up the superficial muscle of the upper thigh. The nerve was cut proximally just below the spinal ganglia, and distally just above the knee joint. The sciatic nerve was sectioned in proximal and distal segments and then soaked in fixative solution. Cross and longitudinal sections of the sciatic nerves were then prepared for electron microscopy. For the central nervous system, the spinal cord was removed and cord regions (cervical, thoracic, and lumbar) selected and fixed as described above. In all cases, tissue was postfixed in 2% osmium tetroxide in NaCac, stained en bloc with 2% uranyl acetate, dehydrated using a graded ethanol series and embedded in Epon-Araldite resin. Thin sections were cut with a diamond knife using a Leica EM UC6 ultramicrotome (Leica Microsystems, Inc, Bannockburn, IL), collected on copper grids and stained with 2% uranyl acetate and lead citrate. Cells were observed in a JEM 1230 transmission electron microscope (JEOL USA Inc., Peabody, MA) at 110 kV and imaged with an UltraScan 4000 CCD camera & First Light Digital Camera Controller (Gatan Inc., Pleasanton, CA).

### Quantitative analysis and statistic methods

*Sciatic nerve* - four sections and thirty six microscope fields in each section were randomly selected for quantitative analysis and >9 images examined per section. Quantification of hypomyelination was performed as described previously (Little and Heath, 1994). The myelinated axon and total fiber circumferences, as well as axon diameters, were measured by digitally tracing around the perimeters of the inner and outer layers of the myelinated

fiber using ImageJ software (NIH). The g-ratio was calculated by dividing the inner circumference of the axon (without myelin) by the outer circumference of the total fiber (including myelin). For the quantification of the g-ratio, a total of 100 myelinated fibers were measured. Data were analyzed using Excel software and statistical differences were carried out using the Student's *t*-test ($p < 0.05$).

For quantification of myelination in spinal cord axons, three sections and fifteen electron microscopy fields were randomly selected from the anterolateral columns of each region, and all images from both comparable areas were examined. A total of 204 myelinated fibers from the wild type and null mice were measured. Measurements were performed independently by three different investigators blinded to the genotypes of the mice. The g-ratios of myelinated fibers from the white matter were calculated as described above. Data were analyzed using Excel software and statistical differences were carried out using the Student's *t*-test ($p < 0.05$).

## Behavioral analysis

Age-matched wild-type, *Lgi1* heterozygote mutant and *Lgi1* null mutant littermates (P15-P18) were analyzed using sensory and motor behavioral tests including the hot plate, tail flick, tube running and wire-hanging tests. Mice were grouped with lactating females and maintained at room temperature on a 12-h light-dark schedule with food and water provided *ad libitum*. All experiments were performed in the light phase and approved by Animal Care and Use Committee of Medical College of Georgia.

**Thermal stimulus assay—**For three consecutive days preceding the experiments, mice (8.3 ± 1.2 g) were placed on a hot plate platform maintained at room temperature for a 15 min adaptation period (Silva et al, 2003). The day of the experiment mice were gently placed onto a 55 ± 1°C hot plate and the latency of response to the thermal stimulus (licking, jumping or hindpaw flicking) from the heated surface were manually recorded with a chronometer. The latency of the response from each mouse was recorded to the nearest millisecond (s). After testing, the mice were immediately removed from the hot plate and returned to their home cages.

**Tail flick test –—**The tail flick test was modified from a previous method (Dewey et al 1970). The basal reaction time of mice to radiant heat was recorded by placing the tip of the tail on the radiant heat source (water bath at 55 ± 1°C). The withdrawal of the tail from the heat (flicking response) was taken as the end point. The latency of response of each mouse was manually recorded with a chronometer to the nearest millisecond (s).

**Track running assay—**To assess motor coordination and balance, we performed a track running test (Carter et al, 1999), which measures the ability of mice to navigate down a narrow tube to reach a dark box. The tube (91.5 cm long, 7.5 cm in diameter) was placed horizontally on the bench surface and each mouse was challenged five times (trials) to reach the box. During training and experimental runs mice were placed at the start of the tube and the time taken to reach the dark box was recorded. A maximum of 60 s was allowed for each trial. The number of successful trials (ST) was also recorded and scored as follow: 0 - if the mouse failed to reach the end of the tube, 1 - if the mouse succeeded in only 1 trial, 2 - if it succeeded in only 2 trials, etc.

**Wire-hanging test—**To measure neuromuscular strength, we performed the wire-hanging test as described previously (Ogura et al, 2001). The apparatus was a flexible stainless steel wire (20 cm long; 2 mm in diameter) placed on support towers 35 cm above a flat surface. Mice were placed on the wire with the two forepaws at a point midway between the supports

and observed for 60 s. Each mouse was challenged on five different attempts. Each attempt was scored as follows: 0 - if the mouse fell off the wire, 1 - if the mouse hung with the two forepaws, 2 - if the mouse hung with the two forepaws and attempted to escape, 3 - if the mouse hung with the two forepaws and one of the hind paws, 4 - if the mouse hung with all 4 paws, and 5 - if the mouse escaped to one of the vertical supports.

### Primary Schwann cell culture

Sciatic nerves were dissected from a P17 mice under aseptic conditions and collected in serum free media. The minced nerves were dissociated in 0.125% trypsin (HyClone) and 0.01% collagenase D (Roche) for 1 hour at 37°C. Cells were cultured for 5 to 10 days in MEM/EBSS supplemented with 10% FBS, Penicillin-Streptomycin, and 100 ng/mL NGF (BD Biosciences). At confluence, cells were dissociated in 0.25% trypsin and plated for 1 hour at 37°C to allow endoneurial fibroblast to attach to the culture dish. Since Schwann cells take longer to attach, the suspension cells were collected, centrifuged and plated in Poly-L-Lysine coated coverslips. The purity of the cultured Schwann cells was typically 90%.

### Immunocytochemistry

Cultured Schwann cells were fixed overnight in 4% paraformaldehyde, rinsed with PBS, permeabilized in 0.1% Triton-X-100/PBS at room temperature for 10 min and blocked in 3% ovalbumin at room temperature for 30 minutes. Incubation with the primary antibodies was performed overnight at 4°C with rabbit polyclonal GFP (1:200; Abcam), rabbit polyclonal PMP22 (1:200; Abcam), and rabbit polyclonal to Lgi1 (1:200; Abcam) in blocking buffer (3% ovalbumin). Donkey anti-rabbit IgG-Cy2 (Jackson Immunoresearch) was used at 1:200 dilution for 30 minutes at 37°C. Nuclei were countstained with 5μM Hoechst (Sigma). Cells were examined under Zeiss confocal microscope and images were processed using Adobe Photoshop.

## RESULTS

We have recently reported that null mutant mice for the *Lgi1* gene exhibit myoclonic seizures with a characteristic onset of 16–20 days after birth (Yu et al 2010). During routine analysis of littermates with different genotypes, we noted a distinct lethargy in the null mutant mice prior to the onset of seizures compared with the wild type and heterozygous mutant mice. To compare age-matched null mice with wild type littermates, therefore, it was necessary to perform the analyses before day P19. The MICER targeting vectors (Adams et al 2004) used to generate the *Lgi1* null mice (Yu et al 2010) carry the agouti and tyrosinase coat color markers. When backcrossed onto an albino background, this resulted in the *Lgi1* null mice having a cream colored coat with dark ruby eyes compared with the wild type, which had pink eyes and a white coat. The heterozygotes had a white coat with dark ruby eyes. These phenotypic markers allowed easy identification of the different genotypes. To evaluate neurological functions in the three different *Lgi1* genotypes we performed a series of tests to assess impaired sensory and motor functions.

### Assessment of neurological function

Abnormal myelination has neurological consequences including impaired sensory and motor functions. According to Hu et all (2006), although there is no neurological test specific for myelin pathology, nociception tests, neuromuscular strength, and coordination and balance assessments have been used to examine the effect of myelin gene mutations on sensory and motor activity.

To evaluate pain sensitivity, we compared pain thresholds in *Lgi1*-null and wild-type mice using two different thermal methods of nociceptive activity. When placed on the surface of a hot plate, mice lift their paws and lick them or jump in response to the applied heat. The reaction time to paw withdrawal is a measure of their sensitivity to pain. In addition, when the tail is placed on a radiant heat source, mice will normally flick the tail to avoid the stimulus. The reaction time to withdrawal of the tail from the heat source is again a measure of its sensitivity to pain. Both responses involve central nervous system sensory pathways. In these experiments, we found no difference between the wild-type and *Lgi1*-null mice in either the hot plate assay or the tail-flick assay. These data demonstrate that sensory pathways are apparently conserved in *Lgi1*-null mice, since their reaction time was similar to those of wild-type and heterozygous mice (Figure 1).

**Motor activity—**To examine the effect of LGI1 on motor coordination as well as neuromuscular strength, we performed the track running and wire-hanging tests. When normal mice are placed at one end of a cardboard tube leading to a dark box they will run the length of the tube to safety. The time taken to traverse this course is a measure of their locomotor activity. The frequency with which they reached the box within the 60 s time period is defined as a successful trial (ST). Both the wild type and heterozygous mice easily passed down the tube. Average time taken by the wild type mice (N = 6 mice, 30 trials) was 26.80 ± 3.9 seconds (speed of movement 3.96 ± 0.7 cm/s) with an ST score of 4.16 ± 0.4. Heterozygous mutant mice (N = 7 mice, 35 trials) traversed the tube in 30.85 ± 5.2 seconds with a speed of movement 3.46 ±0.5 cm/s and an ST score of 3.28 ± 0.3 ($p > 0.1$). In contrast, only 2/9 null mutant mice successfully exited the tube in the allotted time and then only in one or two trials respectively (ST = 0.33 ± 0.2). Of the three successful attempts by these mice the average time to complete the trial was 49 ± 2.8 s with an average speed of 1.8 cm/s. These data confirm that the *Lgi1* null mutant mouse is hypoactive and hypokinetic compared to the wild type and heterozygote littermates (Figure 1C).

**Neuromuscular strength—**In the wire hanging test the *Lgi1* null mutant mice performed poorly, frequently falling off the wire compared to their wild type and heterozygous littermates. Using the scoring procedure outlined in the Materials and Methods section, the null mutant mice scored 1.78 ± 0.3 (N = 10, trials = 50), whereas the wild type and heterozygous littermates scored 3.55 ± 0.4 (N = 7, trials = 35) and 2.94 ± 0.3 (N = 10, trials =50), respectively ($p < 0.05$) (Figure 1D). There was no difference in body weight between the genotypes demonstrating that *Lgi1* null mice possess reduced grip strength to support their body weight.

## Analysis of myelination in the peripheral and central nervous systems

Myelin is typically a compacted membrane sheath that surrounds axons and promotes rapid propagation of electrical signals along axons and nerves in the central and peripheral nervous systems and helps prevent the impulses from leaving the axon. Decreased myelination (hypomyelination) is typical of some neuropathies which are characterized clinically by hypotonia, muscle weakness, and very slow nerve conduction velocities. The comparative analysis of the general behavior of littermates described above demonstrated that the null mutant mice were clearly more lethargic and hypokinetic from birth compared with the heterozygous and wild type mice. This lethargy possibly indicated that these mice had reduced nerve conductance related to myelination abnormalities in the peripheral nervous system. We therefore, analyzed the sciatic nerves from null mutant, heterozygote and wild type littermates using EM analysis. Gross visual analysis of the sciatic nerves under EM suggested two specific abnormalities; there appeared to be an increased proportion of axon fibers showing hypomyelination in the null mice compared with wild type mice (Figure 2A and B) and there was also an increased incidence of axon fibers that

showed a comparatively looser organization of the myelin layers of the axons. Degenerating axons were also more frequently seen in the *Lgi1*-null mice (Figure 2C). Many axons in the mutant mice showed normal Schwann cell associations, suggesting proper radial sorting and the number of myelinated axons in the wild type (90%) and null cells (82%) were similar suggesting no difference in myelin initiation.

To evaluate the degree of myelination in sciatic nerves from these mice, we generated g-ratios (Little and Heath, 1994) to compare myelin thickness between wild type and null mice. The g-ratio is a standard ultrastructural analysis that provides a reliable index of myelination that is independent of axonal diameter (Michailov et al, 2004). Using ImageJ software, the axon area was measured and the diameter was calculated using: axonal diameter = $2 \times \sqrt{}$(axonal area/$\pi$). Similarly, fiber diameter was calculated using: fiber diameter = $2 \times \sqrt{}$(fiber area/$\pi$). The g-ratio is defined as axonal diameter/fiber diameter. G-ratios from 100 axons each from the normal and null mice were compared. In wild-type mice, the average g-ratio was 0.48 ± 0.01 compared with 0.56 ± 0.006 for age-matched *Lgi1*-null mice, demonstrating a significantly ($p$ = 2.7404E-18) thinner myelin sheath in the null mouse compared to the wild-type littermate controls (Figure 2D). Myelin sheath thickness was reduced in null mice for all axonal diameters (Figure 2D). Myelin sheath thickness in sciatic nerves of heterozygous *Lgi1* mutant mice was intermediate between age-matched wild-type and null mutant mice (Figure 2D). In the g-ratio analysis, even when the grossly degenerating fibers were excluded, there was still a significant difference between all genotypes. These observations support the idea that the lethargic phenotype in the null mutant mice is a consequence of hypomyelination.

To determine whether loss of LGI1 function also occurred in the central nervous system, we analyzed myelination in the white matter of the spinal cord (Figure 3). In this analysis, areas from the anterolateral column were analyzed from age-matched wild-type and null littermates. Axons were classified into two different size categories based on myelin sheath thickness: 0 – 2 μM (small fibers) and > 2 μM (large fibers). In this analysis (Figure 3), the g-ratios were significantly ($p$ < 4.97432E-12) smaller in the wild-type (0.69 ± 0.004) compared with the *Lgi1* null mutant littermates (0.74 ± 0.005). Although the null mutant mice showed significantly increased g-ratios when all axons were included, this difference was more pronounced for the smaller fibers (Figure 3C).

## LGI1 is expressed in Schwann cells and oligodendrocytes

The hypomyelination seen in the CNS and PNS of the mutant null mice implies that Schwann cells and oligodendrocytes express LGI1. To evaluate expression in Schwann cells we first used the BAC transgenic mouse described by Head et al (2007), which provides a knock-in GFP reporter for endogenous LGI1 expression. Schwann cells were isolated from the sciatic nerve from E17 mice and enriched from these cultures after 6–10 days (see Materials and Methods). Schwann cells are readily detected in the cultures as spindle shaped cells. When stained for the presence of the GFP reporter (Supplemental figure 1), Schwann cells fluoresce strongly suggesting the expression capacity for LGI1. When Schwann cells were similarly isolated from sciatic nerves from Lgi1 mutant null and wild type mice, and stained with an anti-LGI1 antibody (supplemental figure 1), it was also clear that Schwann cells from the wild type mouse expressed LGI1 but that the Schwann cells from the mutant null mice did not. The spindle shaped cells were confirmed to be Schwann cells using the PMP22 Schwann cell-specific protein marker.

To confirm LGI1 expression in oligodendrocytes, we analyzed gene expression profiles from these cells in the Gene Expression Omnibus (GEO) at www.ncbi.nlm.nih.gov. From this analysis LGI1 was clearly expressed in oligodendrocytes and their precursors (e.g entry GDS2380).

### Axon fibers from the null mice show distinct neuropathology

Our initial review of the axon fibers in the sciatic nerves of the null mutant mice suggested a distinct degeneration of the myelin fibers surrounding many axons. Examples of the ultrastructural abnormalities of the myelin sheaths seen in axons in the PNS from the null mice are shown in figure 4. Although the appearance of disorganization was seen throughout the sciatic nerve, there were small clusters where myelin sheath breakdown was more prevalent in *Lgi1*-null mice. In addition, in the wild type mice, there was little or no evidence of mitochondrial clustering, which often precedes axonal degeneration, whereas in the null mice frequent examples were observed (Figure 4C). Other features of terminal neuronal degeneration, such as breakdown of the myelin packing and electron-dense cytoplasm which separates from the axolemma (Figure 4B), was shown to occur only in the axons derived from null mutant mice. These observations suggest that loss of LGI1 function has profound consequences for myelin formation and survival of axons in the PNS.

### Analysis of myelin compaction in the PNS

The hypomyelination seen in the null mutant mice could be due to either a reduced number of myelin layers or denser compaction of the myelin layers. To investigate the compaction of the myelin layers, we measured the interperiod lines and periodicity in the myelin sheath from wild type and mutant mice. As shown in figure 5, there is a significant reduction both in the number of myelin lamelli as well as their compaction in the mutant mice. The interperiod lines, or periodicity, of the myelin sheath (Figure 5) is significantly decreased in *Lgi1*-null mice ($p < 0.05$), which showed myelin periodicity of $32.3 \pm 2$ rim ($N = 27$) while the wild-type showed a periodicity of $39.2 \pm 3$ rim ($N = 17$). These data demonstrate that the hypomyelination (increased g-ratio) observed in *Lgi1*-null mice was the result of a decrease in the number of myelin wrappings.

## Discussion

In this study we demonstrate that poor locomotor activity and neuromuscular strength in mice deficient for LGI1 is due to hypomyelination in the peripheral nervous system. A significant, but less extreme hypomyelination was also seen in the heterozygous mutant mice. These mice also showed marginally worse locomotor activity and neuromuscular strength compared with the wild type mice, although it was not statistically significant. These phenotypes have not been reported in ADPEAF patients although, as in mice, a mild reduction in myelination may not have immediately obvious consequences. The same was true in the *Lgi4* mutant heterozygotes (Bermingham et al, 2006), where the heterozygous mutants appeared normal. The hypomyelination in *Lgi1* mutants results from reduced numbers of myelin wrappings, which suggests, as LGI4, that LGI1 appears to have a role in Schwann cell myelination function. In our study we also found significant hypomyelination in the central nervous system, although not to the same extent seen in the PNS. This change was not seen in the *Lgi4* mutant mice but suggests that LGI1 may have an important function in oligodendrocytes as well.

The function of the LGI1 protein is still poorly understood, although recent reports implicate it in synapse transmission *in vitro* (Schulte et al 2006) and *in vivo* (Zhou et al 2009, Yu et al 2010, Fukata et al 2006, 2010). LGI1 also interacts with proteins involved in synapse biology, in particular ADAM22 and ADAM23 (Fukata et al 2006, Schulte et al 2006, Sagane et al 2008, Kunapuli et al 2009). Null mutant mice for *Adam22* have also been shown to exhibit hypomyelination in the PNS (Sagane et al 2005) and succumb to seizures. Compared with the *Lgi1* null mutant mice, however, the phenotype in the *Adam22* null appears to be more extreme and also shows many unmyelinated axons resulting in severe ataxia (Sagane et al 2005). Although not specifically examined for hypomyelination, the

*Adam23* null mouse also showed evidence of ataxia (Mitchell et al 2001). ADAM23 has been shown to interact with LGI1 (Fukata et al 2006, SAgane et al 2008, Kunapuli et al 2009) and, in its absence, LGI1 cannot initiate neurite outgrowth (Owuor et al 2009).

*LGI1* is the founding member (Chernova et al 1998) of a family of four genes with high homology (Gu et al 2002, Rossi et al 2003) suggesting a related function. The claw paw (*clp*) phenotype that arose spontaneously in mice (Henry et al 1999) is characterized by limb posture abnormalities and hypomyelination of peripheral nerves. The *Lgi4* gene was subsequently shown to be mutated in these mice (Bermingham et al 2006). *In vitro* studies of *clp/clp* mice showed that Schwann cells had a significantly reduced capacity to myelinate axons, suggesting a disruption of the cross talk between these two cell types. LGI4 was also shown to interact with ADAM22 and ADAM23 (Sagane et al 2008) and the LGI4-ADAM22, ligand-receptor relationship has been described as a paracrine signaling axis in peripheral nerve myelination (Ozkaynak et al 2010). The hypomyelination seen in the *Lgi1* null mice was also very similar to that seen in erbin null mice (Tao et al 2009), another LRR-containing gene. Erbin has been shown to regulate Schwann cell development and myelin formation through the Erbb2/Erbb3 receptor. Erbin and LGI1, as well as several other LRR-containing proteins, have also been shown to have important implications in the formation, differentiation, maintenance and plasticity of neuronal synapses (Ko and Kim 2007).

Myelination is one of the most strictly regulated biological events that occur in development and maturation of the mammalian peripheral and central nervous systems. The demonstration that LGI1 is an important contributor to normal myelination provides the opportunity to improve our understanding of the axon-Schwann and axon-oligodendrocytes cell interactions that regulate this process through a more exhaustive study of its function.

## Supplementary Material

Refer to Web version on PubMed Central for supplementary material.

## Acknowledgments

This work was supported in part by grants from the National Institutes of Health NS046706 (JC)

## REFERENCES

Adams DJ, Biggs PJ, Box T, Davies R, van der Weyden L, Jonkers J, Smith J, Plumb B, Taylor R, Nishijima I, Yu Y, Rogers J, Bradley A. MICER – Mutagenic insertion and chromosome engineering resource. Nature Genet. 2004; 36:867–871. [PubMed: 15235602]

Bermingham JR Jr, Shearin H, Pennington J, O'Moore J, Jaegle M, Driegen S, van Zon A, Darbas A, Ozkaynak E, Ryu EJ, Milbrandt J, Meijer D. The claw paw mutation reveals a role for Lgi4 in peripheral nerve development. Nat Neurosci. 2006; 9:76–78. [PubMed: 16341215]

Carter RJ, Lione LA, Humby T, Mangiarini L, Mahal A, Bates GP, Dunnett SB, Morton AJ. Characterization of progressive motor deficits in mice transgenic for the human huntington's disease mutation. J Neurosci. 1999; 19:3248–3257. [PubMed: 10191337]

Chernova O, Somerville RPT, Cowell JK. A novel gene, *LGI1*, from region 10q24, is rearranged and downregulated in malignant brain tumors. Oncogene. 1998; 17:2873–2881. [PubMed: 9879993]

Dewey WL, Harris LS, Howes JF, Nuite JA. The effect of various neurohumoral modulators on the activity of morphine and the narcortic antagonists in the tail-flick and phenylquinone testes. J Pharmacol Exp Therap. 1970; 175:435–442. [PubMed: 4394803]

Fukata Y, Adesnik H, Iwanaga T, Bredt DS, Nicoll RA, Fukata M. Epilepsy-related ligand/receptor complex LGI1 and ADAM22 regulate synaptic transmission. Science. 2006; 313:1792–1795. [PubMed: 16990550]

Fukata Y, Lovero KL, Iwanaga T, Watanabe A, Yokoi N, Tabuchi K, Shigemoto R, Nicoll RA, Fukata M. Disruption of LGI1-linked synaptic complex causes abnormal synaptic transmission and epilepsy. Proc Natl Acad Sci. 2010; 107:3799–3804. [PubMed: 20133599]

Gu W, Gibert Y, Wirth T, Elischer A, Bloch W, Meyer A, Steinlein OK, Begemann G. Using gene-history and expression analyses to assess the involvement of LGI genes in human disorders. Mol Biol Evol. 2005; 22:2209–2216. [PubMed: 16014869]

Head K, Gong S, Joseph S, Wang C, Burkardt T, Rossi MR, LaDuca J, Matsui S-I, Vaughan M, Hicks DG, Heinz N, Cowell JK. The expression pattern of the LGI1 gene in tissues and organs from BAC transgenic mice demonstrate a neuronal and glial expression pattern as well as other distinct cell types in the adult animal. Mamm Genom. 2007; 18:328–337.

Henry EW, Eicher EM, Sidman RL. The mouse mutation claw paw: forelimb deformity and delayed myelination throughout the peripheral nervous system. J Hered. 1991; 82:287–294. [PubMed: 1652607]

Herranz-Pérez V, Olucha-Bordonau FE, Morante-Redolat JM, Pérez-Tur J. Regional distribution of the leucine-rich glioma inactivated (LGI) gene family transcripts in the adult mouse brain. Brain Res. 2010; 1307:177–194. [PubMed: 19833108]

Hu X, Hicks CW, He W, Wong P, Macklin WB, Trapp BD, Yan R. Bace1 modulates myelination in the central and peripheral nervous system. Nat Neurosc. 2006; 9:1520–1525.

Kalachikov S, Evgrafov O, Ross B, Winawer M, Barker-Cummings C, Martinelli Boneschi F, Choi C, Morozov P, Das K, Teplitskaya E, Yu A, Cayanis E, Penchaszadeh G, Kottmann AH, Pedley TA, Hauser WA, Ottman R, Gilliam TC. Mutations in LGI1 cause autosomal-dominant partial epilepsy with auditory features. Nat Genet. 2002; 30:335–341. [PubMed: 11810107]

Ko J, Kim E. Leucine-rich repeat proteins of synapses. J Neurosci Res. 2007; 85:2824–2832. [PubMed: 17471552]

Kunapuli P, Jang G, Kazim L, Cowell JK. Mass Spectrometry identifies LGI1-interacting proteins that are involved in synaptic vesicle function in the human brain. J Molec Neurosci. 2009; 39:137–143. [PubMed: 19387870]

Little GJ, Heath JW. Morphometric analysis of axons myelinated during adult life in the mouse superior cervical ganglion. J Anat. 1994; 184:387–398. [PubMed: 8014130]

Michailov GV, et al. Axonal neuregulin-1 regulates myelin sheath thickness. Science. 2004; 304:700–703. [PubMed: 15044753]

Mitchell KJ, Pinson KI, Kelly OG, Brennan J, Zupicich J, Scherz P, Leighton PA, Goodrich LV, Lu X, Avery BJ, Tate P, Dill K, Pangilinan E, Wakenight P, Tessier-Lavigne M, Skarnes WC. Functional analysis of secreted and transmembrane proteins critical to mouse development. Nat Genet 2001. 2001; 28:241–249.

Nelis E, Timmerman V, De Jonghe P, Van Broeckhoven C, Rautenstrauss B. Molecular genetics and biology of inherited peripheral neuropathies: a fast-moving field. Neurogenetics. 1999; 2:137–148. [PubMed: 10541586]

Ogura H, Aruga J, Mikoshiba K. Behavioral abnormalities of Zic1 and Zic2 mutant mice: Implications as models for human neurological disorders. Behav Genet. 2001; 31:317–324. [PubMed: 11699604]

Ottman R, Risch N, Hauser WA, Pedley TA, Lee JH, Barker-Cummings C, Lustenberger A, Nagle KJ, Lee KS, Scheuer ML, et al. Localization of a gene for partial epilepsy to chromosome 10q. Nat Genet. 1995; 10:56–60. [PubMed: 7647791]

Owuor K, Harel NY, Englot DJ, Hisama F, Blumenfeld H, Strittmatter SM. LGI1-associated epilepsy through altered ADAM23-dependent neuronal morphology. Mol Cell Neurosci. 2009; 42:448–457. [PubMed: 19796686]

Ozkaynak E, Abello G, Jaegle M, van Berge L, Hamer D, Kegel L, Driegen S, Sagane K, Bermingham JR Jr, Meijer D. Adam22 is a major neuronal receptor for Lgi4-mediated Schwann cell signaling. J Neurosci. 2010; 30:3857–3864. [PubMed: 20220021]

Rossi MR, Huntoon K, Cowell JK. Differential expression of the LGI and SLIT families of genes in human cancer cells. Gene. 2005; 356:85–90. [PubMed: 16000246]

Sagane K, Hayakawa K, Kai J, Hirohashi T, Takahashi E, Miyamoto N, Ino M, Oki T, Yamazaki K, Nagasu T. Ataxia and peripheral nerve hypomyelination in ADAM22-deficient mice. BMC Neurosci. 2005; 6:33. [PubMed: 15876356]

Sagane K, Ishihama Y, Sugimoto H. LGI1 and LGI4 bind to ADAM22, ADAM23 and ADAM11. Int J Biol Sci. 2008; 4:387–396. [PubMed: 18974846]

Scherer SS, Wrabetz L. Molecular mechanisms of inherited demyelinating neuropathies. Glia. 2008; 56:1578–1589. [PubMed: 18803325]

Schulte U, Thumfart JO, Klöcker N, Sailer CA, Bildl W, Biniossek B, Dehn D, Deller D, Eble S, Abbass K, Wangler T, Knaus HG, Fakler B. The epilepsy-linked Lgi1 protein assembles into presynaptic Kv1 channels and inhibits inactivation by Kvbeta1. Neuron. 2006; 49:697–706. [PubMed: 16504945]

Senechal KR, Thaller C, Noebels JL. ADPEAF mutations reduce levels of secreted LGI1, a putative tumor suppressor protein linked to epilepsy. Hum Mol Genet. 2005:1613–1620. [PubMed: 15857855]

Silva J, Abebe W, Sousa SM, Duarte VG, Machado MIL, Matos FJA. Analgesic and anti-inflammatory effects of essential oils of eucalyptus. Journal of Ethnopharmacology. 2003; 89:277–283. [PubMed: 14611892]

Sirerol-Piquer MS, Ayerdi-Izquierdo A, Morante-Redolat JM, Herranz-Pérez V, Favell K, Barker PA, Pérez-Tur J. The epilepsy gene LGI1 encodes a secreted glycoprotein that binds to the cell surface. Hum Mol Genet. 2006; 15:3436–3445. [PubMed: 17067999]

Tao Y, Dai P, Liu Y, Marchetto S, Xiong WC, Borg JP, Mei L. Erbin regulates NRG1 signaling and myelination. Proc Natl Acad Sci. 2009; 106:9477–9482. [PubMed: 19458253]

Yu YE, Wen L, Silva J, Li Z, Head K, Sossey-Alaoui K, Pao A, Mei L, Cowell JK. Lgi1 null mutant mice exhibit myoclonic seizures and CA1 neuronal hyperexcitability. Hum Mol Genet. 2010 In Press.

Zhou YD, Lee S, Jin Z, Wright M, Smith SE, Anderson MP. Arrested maturation of excitatory synapses in autosomal dominant lateral temporal lobe epilepsy. Nat Med. 2009; 15:1208–1214. [PubMed: 19701204]

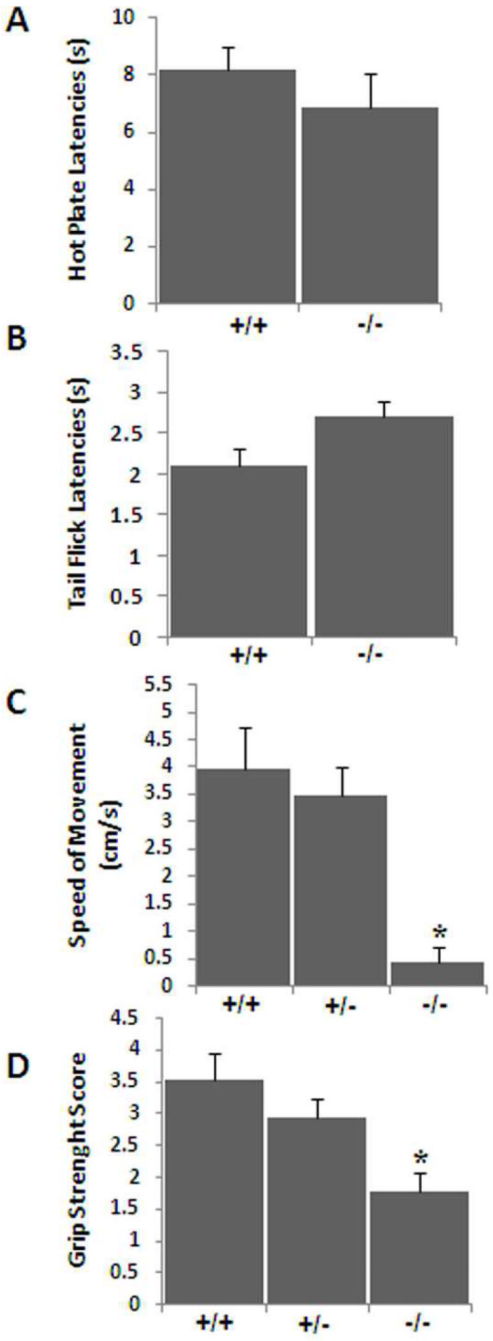


**Figure 1.**

In an analysis of pain sensitivity in *Lgi1* null mice, the latency in response to thermal stimulation was recorded (A) in a hot plate assay and (B) in the tail flick assay. No significant difference was observed between the two groups in either case demonstrating preservation of sensory functions in *Lgi1* null mice. To analyze motor activity and neuromuscular strength in *Lgi1* null mice, P16 to P18 mice were trained to walk down a narrow tube to reach a dark box (C) and muscular strength was performed using the wire-hanging test (D). *Lgi1* null mutant mice showed a significantly reduced locomotor activity

(C) and reduced grip strength (D) (* $p < 0.05$). No significant difference was observed between the wild type and heterozygous mutant animals in these two assays.

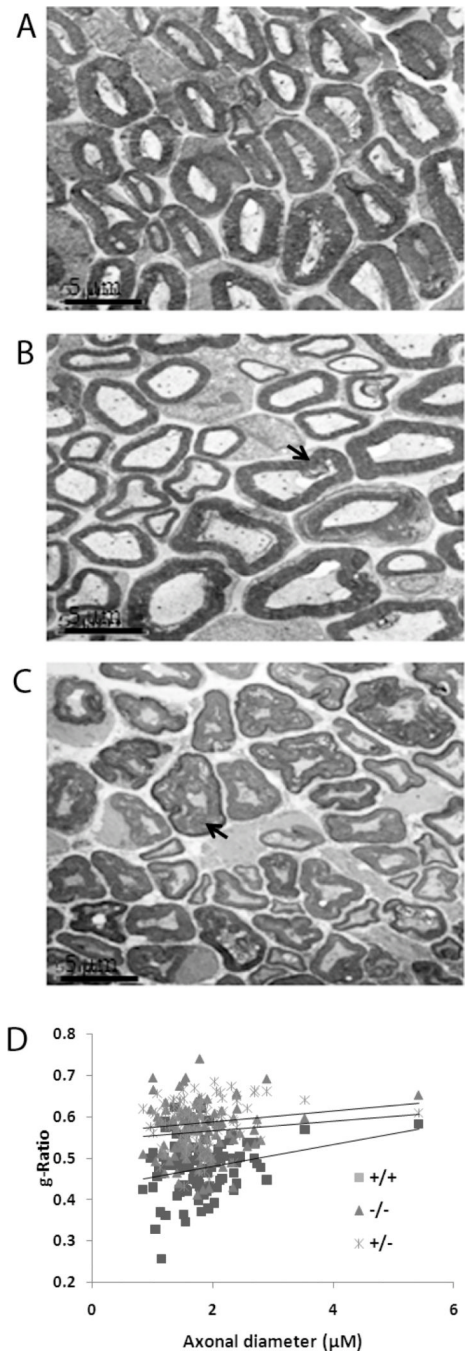


**Figure 2.**

Representative electron micrographs show cross-sections of sciatic nerves from wild type (A) and *Lgi1*-null (B, C) littermates at P17. Focal myelin whorls (arrowheads in B) and degenerating axons (arrowheads in C) are visible in null mutant mice. [scale bar 5µm]. G-ratios from sciatic nerves (D) from wild-type, heterozygous and null mutant mice at P17 and P18 show significantly reduced myelination in null mice. Data represent the mean ± S.E.M. for 100 myelinated fibers from each group ($p < 0.05$).

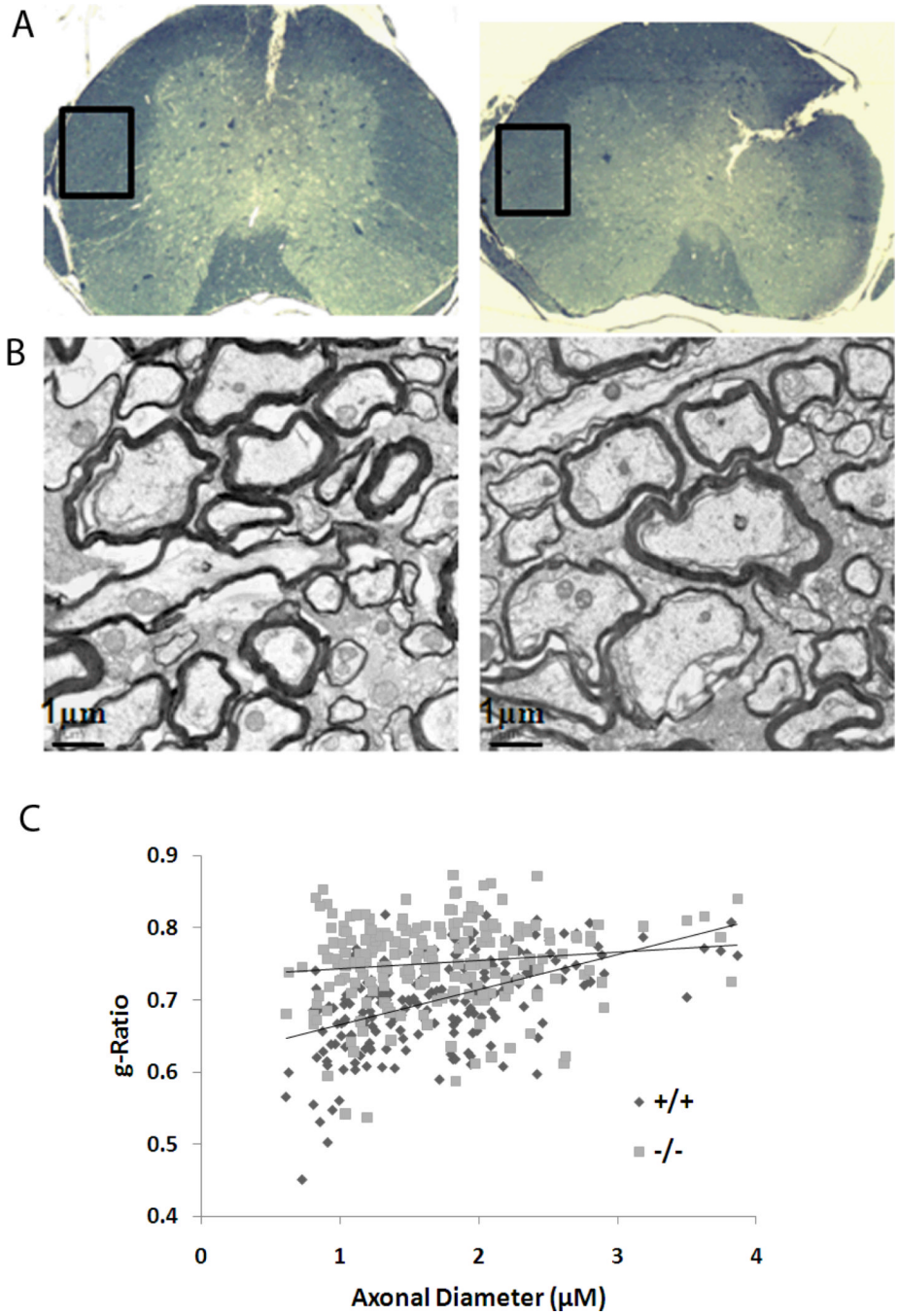


**Figure 3.**

Ultrastructural analysis of the spinal cord axon fibers. (A) A representative cross-section of the spinal cord showing the location of the white matter that was used from the anterolateral columns and prepared for electron microscopy. (B) Representative electron micrographs from wild-type (left) and *Lgi1* null mice (right) showing hypomyelinated axons. [scale bar 1μm]. G-ratio analysis demonstrates a significant hypomyelination in the null mice compared with the wild type mice, particularly in the smaller axons.

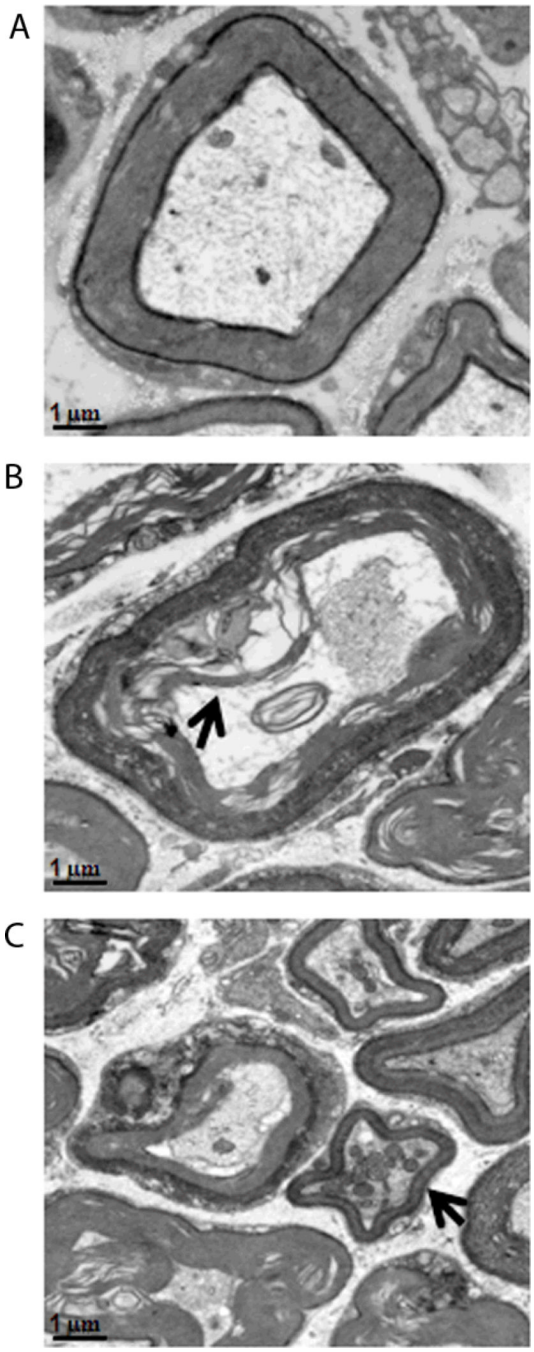


**Figure 4.**
Utrastructural abnormalities of the myelin sheaths in *Lgi1* null mutant mice (B, C) compared with normal mice (A). Evidence of neuronal degeneration includes myelin sheath break down (B) with electron-dense cytoplasm (arrowhead in B) and mitochondrial clustering (arrowhead in C). [scale bar 1µm].

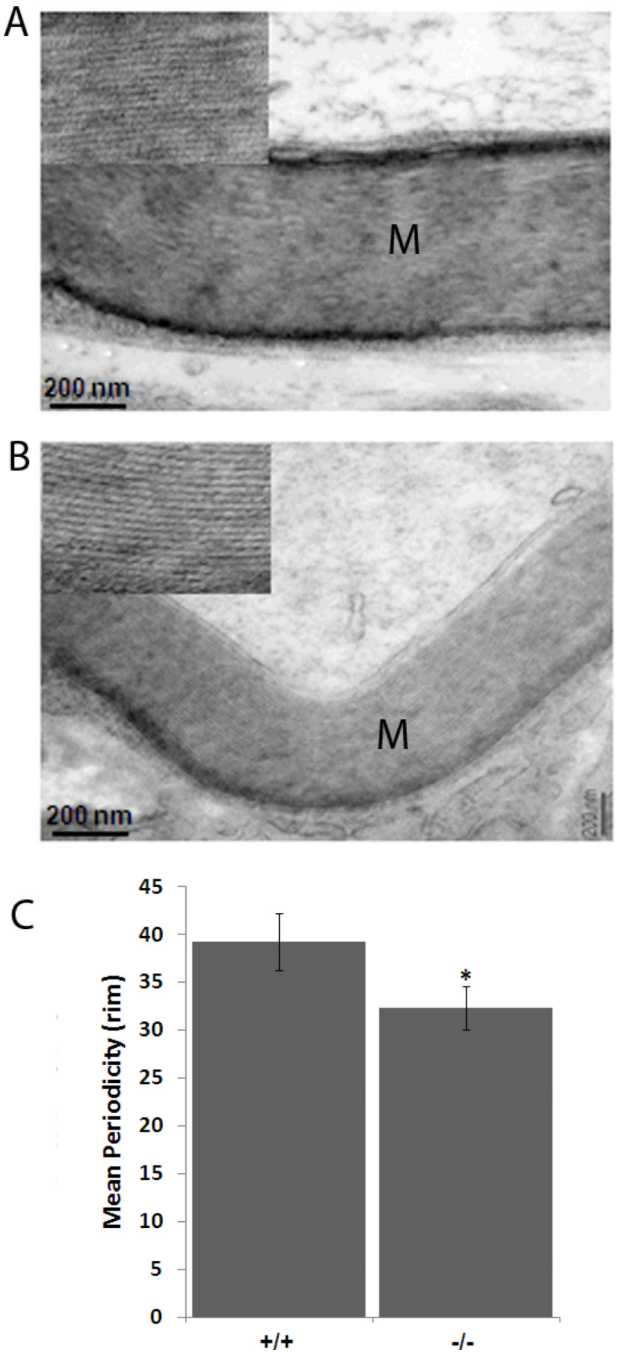


**Figure 5.**

Analysis of myelin periodicity in normal and *Lgi1* null mutant mice. Compared with normal mice (A), reduced myelin compaction is seen in the sciatic nerve of *Lgi1*-null mice (B), accompanied by differences in myelin sheath thickness (M) [scale bar 200nm]. In (C) the data represent the mean ± S.E.M. from 17 and 27 myelinated fibers respectively for each group. *$p < 0.05$.